DISTRIBUTED ALGORITHMS FOR ELECTRIC VEHICLE CHARGING

by

AKSHAY MALHOTRA

Presented to the Faculty of the Graduate School of

The University of Texas at Arlington in Partial Fulfillment

of the Requirements

for the Degree of

MASTER OF SCIENCE IN ELECTRICAL ENGINEERING

THE UNIVERSITY OF TEXAS AT ARLINGTON

December 2015

To my parents Subir and Manisha Malhotra

who have helped and guided me at every moment in my life.

ACKNOWLEDGEMENTS

A lot of people have contributed to the success and completion of my thesis, from whom I have learnt a lot of lessons which will be quite invaluable for me in my future pursuits.

Firstly, I would like to thank my supervising Professor; Dr. I. D. Schizas for his mentor-ship, invaluable pieces of advice during the course of my research. Dr. Schizas was there to encourage and guide me throughout the course of my research at UTA. I would also like to thank him for giving me the opportunity to conduct this research work under him and for the financial assistance that he provided me with.

I wish to thank Dr. Ali Davoudi and Dr. Giulio Binetti who co-advised my research work and helped me improve my research and writing skills. I am also thankful to Dr. Manry for taking out time out of his busy schedule to be on my thesis defense committee.

I would also like to extend my appreciation to my other researchers in our group; Jia Chen and Guohua Ren for their support, encouragement and for the helpful discussions we had about our work.

November 23, 2015

ABSTRACT

DISTRIBUTED ALGORITHMS FOR ELECTRIC VEHICLE CHARGING

AKSHAY MALHOTRA, M. Sc.

The University of Texas at Arlington, 2015

Supervising Professor: Ioannis D. Schizas

Coordinated charging of plug-in electric vehicles (PEVs) can effectively mitigate the negative effects imposed on the power distribution grid by uncoordinated charging. Simultaneously, coordinated charging algorithms can accommodate the PEV user's needs in terms of desired state-of-charge and charging time. In this work, the problem of tracking an arbitrary power profile, by coordinated charging of PEVs, is formulated as a discrete scheduling process, while accounting for the heterogeneity in charging rates and restricting the charging to only the maximum rated power. Then, a novel distributed algorithm is proposed to coordinate the PEV charging and eliminate the need for a central aggregator. It is guaranteed to track, and not exceed, the power profile imposed by the utility, while maximizing the user convenience. A formal optimality analysis is provided to show that the algorithm is asymptotically optimal in the case of homogeneous charging, while it has a very small optimality gap for the heterogeneous case.

The work also discusses techniques for achieving aggregate load profiles with minimum variance and peak in both centralized and decentralized settings. A theoretical analysis that proves that peak minimization is inherently achieved as part of an variance minimization process has also been presented.

The impact of interrupted and uninterrupted electric vehicle charging on the aggregated load profile has been explored. The variance of the aggregate load profile is used as the metric for measuring valley filling capability of the scheduling scenarios. It is shown, that for low penetration levels (up to 30%), interrupted charging strategies result in considerably lower variance values on the aggregated load profile as compared to the uninterrupted case. It is also shown that the policy used for deciding the PEV priority for scheduling has almost no impact on these variance values. All the proposed algorithms and the related analysis are accompanied by numerical simulations under realistic charging scenarios.

TABLE OF CONTENTS

LIST OF ILLUSTRATIONS

LIST OF TABLES

CHAPTER 1

INTRODUCTION

The Use of Plug-in Electric Vehicles (PEV) has been extensively promoted in the last few years as an sustainable alternative to the fossil fuel based vehicles. These vehicles are the building blocks of a transportation electrification paradigm and bring along with them the promise of reduction in pollution, global warming and our dependence on the fossil fuels [2, 3].

But the migration to PEVs comes at the cost of an increased power demand. Studies by National Renewable Energy Laboratory (NREL) [4, 5] predict significant impact on the power system with large-scale deployment of PEVs in the uncoordinated charging case. It has been estimated that even in the case of just 20-30% of the current vehicles being replaced by PEVs, uncoordinated charging would result in a steep increment in the peak power requirements accommodating which would require setting up of new power plants. Besides the increased power demand, such an increase in the PEV numbers can have adverse effects on the power grid in the form of transmission loss, and stress on distribution transformers [4, 6–9]. A strategy to resolve this problem would be to coordinate and schedule the charging of the PEVs in such a way that the charging load is disseminated in a smart way to periods of the day when the overall power requirement is low.

1.1 Background on Charging Strategies

The charging strategies can be examined from two viewpoints, the user's or the utility's. For the user, the convenience of charging is the primary concern. A user wants to achieve a desired state-of-charge (SOC) within self defined time limitations. This user con-

venience can be quantified as a function of battery capacity and charging time. In [1] a weighting function, where the weights hyperbolically increase with the SOC and time remaining for plug off has been discussed. Another important factor for identifying a charging schedule is the power price. Since the cost of electricity is different at different periods during the day, the user may prefer to charge the PEV during the time periods associated with lesser power price. On these lines, [10] uses a weighing function that prioritizes the reduction in the cost for charging and [11] utilizes the charging cost and the CO2 emissions as the parameters for scheduling the vehicle charging process. A weighted sum of all the parameters, the SOC, remaining time and energy price, considered in a normalized fashion has been proposed in [12]. Observing the charging situation from the the utility's perspective, it is important to reduce the variance of the aggregate load profile seen by the utility or the grid [13, 14]. In [15], the authors minimize the peak of the aggregate load profile in addition to the variance.

1.2 Tracking Target Load Profiles

In the last few years, another line of the charging algorithms that aim at tracking a specified a target load profile have been introduced. The peak of the base load profile is used as the target load in [1]. In [14] a valley filling approach is presented, the formulation is later extended to track a given target profile by modifying the objective function to reduce the gap between the the current load and the target load profile. A similar approach towards using the gap between the current load and the target load as the cost function has been discussed in [16]. A decentralized approach towards building and tracking a valley filling profile has been given in [17]. A model predictive control approach, that can be used for tracking has been given in [18]. The discussions in the aforementioned papers provide good insight towards the objective of tracking generic target profiles, but also reveal many

associated drawbacks that limit their applicability due to the assumptions made with regard to the charger technology, decentralized and distributed implementation and guaranteed tracking performance.

1.2.1 Discrete Charging

Often-neglected practical aspects in coordinated charging of PEVs include the limitation of charger technologies and the heterogeneity of the charging process. Most charging schemes consider a continuous charging scenario, e.g., [11, 12, 14] to name a few, where the PEVs can withdraw any power from the grid. However, in practice PEVs are charged with power electronics chargers with given power ratings. Discrete charging scenarios can be formulated as a scheduling problem at the charger's maximum power rating. The on/off switching behavior of discrete charging process may potentially allow the battery some cool off time and mitigate rapid temperature rise, an important factor for battery lifetime longevity [19]. Very few existing works discuss heterogeneous charging scenarios, e.g., [1, 15, 20–24]. In general, heterogeneous coordinated charging of PEVs, with discrete charging rates, is largely unexplored.

1.2.2 Interrupted and Uninterrupted Charging

Another important parameter related to the charging technology is whether the PEV is charged continuously, uninterrupted, or during discontinuous charging intervals, as an interrupted charging process. In the interrupted charging scenario (also referred to as on-off charging [13]), a PEV is charged at discrete time-slots that may be separated by idle slots. In the uninterrupted charging scenario, the PEVs are charged continuously until they obtain their desired state of charge (SOC) [15]. The uninterrupted charging process is more constrained in nature since once a PEV starts charging, it continues until the PEV attains

the desired state of charge. This behavior can potentially increase the variance or even the peak of the aggregate load profile.

1.2.3 Decentralized and Distributed Frame work

Existing decentralized charging strategies distribute the computational overhead from the central aggregator to the PEVs, with a hierarchical, tree-like, communication topology. In [1], a two-layer hierarchical structure is considered, where sub-aggregators (SAs) accumulate data from a set of PEVs and report them to the central aggregator constraining the power at both layers. In [25], a layered structure, with constraints accounting for the entire distribution grid, is considered. The algorithms with a central aggregator need a high level of network connectivity, and require high-bandwidth communication links to exchange data. Moreover, in centralized systems, the central aggregator exposes a single point-of-failure, i.e., the failure of the aggregator results in the collapse of the entire system. Similarly, in a hierarchical setup (e.g., [1] and [25]), if the link between a sub-aggregator and the central aggregator collapses, all the PEVs under the SA will be left uncontrolled. Alternatively, distributed charging scenarios replace the central aggregator with multiple sub-aggregators that communicate amongst themselves. Thus, even if a link between two SAs is broken, an alternative communication path connecting the SAs could be used, and the distributed framework is still functional. If a SA goes down, of course the PEVs connected to it will remain uncontrolled. Thus, the main advantage of a distributed architecture is that, since there is no central aggregator as in a hierarchical or centralized setting, not all PEVs end up being uncontrolled in the case of a single failure.

1.2.4 Contributions of the thesis

The main contributions of the thesis are the following:

- The problem of tracking an arbitrary power profile by coordinated charging of PEVs is formalized considering the realistic case of PEVs with different charging rates (*heterogeneous scenario*).
- A novel distributed algorithm coordinates the PEV charging and eliminates the need for a central aggregator. It is guaranteed to track, and not exceed, the power profile imposed by the power utility, while maximizing the user convenience.
- A formal optimality analysis of the proposed algorithm is provided. Asymptotic optimality is proven in the case of homogeneous charging. An optimality gap is derived for the heterogeneous case and shown to be very small in practical settings (ensuring near optimality).
- A centralized and a decentralized approach for achieving a minimum variance valley filling profile, and a formal proof showing that the minimum variance solution guarantees peak minimization.
- The impact of charging interruption on the valley filling (or the variance minimization) potential of the PEV charging algorithms is also discussed.

1.2.5 Outline of Work

The rest of the thesis is organized as follows. Chapter 2 introduces a decentralized PEV charging algorithm that is guaranteed to track a specified target profile. The chapter analyzes the behavior of the algorithm in different realistic scenarios and provides bounds on the optimality of the algorithm. In Chapter 3, a set of centralized and decentralized valley filling algorithms have been presented. The decentralized scheme, in part uses the tracking scheme introduced in Chapter 2 to achieve valley filling behavior. In Chapter 4, the impact of interruption on the PEV charging process has been explored. An interrupted and uninterrupted charging schemes have been compared on the grounds of their effectiveness

in achieving valley filling or the minimum variance solution. Finally, Chapter 5 provides concluding remarks.

CHAPTER 2

DISTRIBUTED POWER PROFILE TRACKING

A distributed, coordinated, PEV charging scheme has been discussed in this chapter. The objective of the charging scheme is to track an arbitrary power profile while maximizing the convenience to the user. The scheme takes into account the heterogeneity in charging rates and considers the ON/OFF charging strategy. The chapter is organized as follows. Section 2.1 describes the layout and the grouping of the PEVs and introduces the primary computational and communication hubs used in the algorithm, the Sub-Aggregators (SAs). Section 2.2 formulates the charging process as a scheduling algorithm and defines a user convenience function based on battery SOC and plug-off time. In Section 2.3, the proposed distributed charging algorithm is discussed and an optimality analysis is provided. Finally in Section 2.4, the algorithm effectiveness is demonstrated by tracking different target profiles and studying different penetration levels. The complexity and scalability of the algorithm has also been discussed.

2.1 System Configuration

PEVs are grouped into K sub groups with 1 Sub-Aggregator (SA) per group. Hence, totally K sub-aggregators are present. Each of the SA communicates only with PEVs in the respective sub group. The SA can also communicate with some of the neighboring SAs. The communication structure is illustrated in Fig. 2.1. The communication between SAs is over high speed data links. The EVs communicate with the SAs over low speed data links. As we will see in Section 2.4, the number of to-and-from communications between SAs is large, but between the SA and the respective set of PEVs within that SA is very restricted

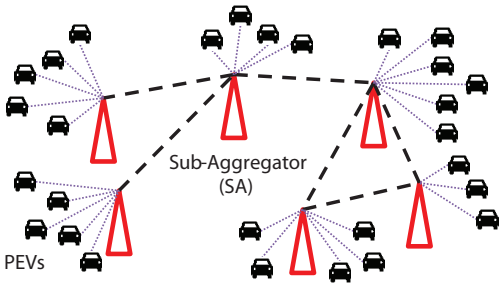

Figure 2.1. Example of a sparse communication network with 6 sub-aggregators..

(only once). Also, the number of SAs is much smaller than the number of EVs and hence equipping inter SA communication with high-speed links is more feasible. This justifies the use of the high speed and low speed data links for intra- and inter- SA communication, respectively.

The Sub-Aggregator (SA) is a power distribution unit and also a local computation and communication hub. Physically, SA can be considered as a power sub-station that receives power from the generation unit (or from the Grid), steps down the voltage and distributes it locally. Due to the capacity of the transformers, there may be a limit on the maximum power that can be made available as input to a sub-station. Hence there are constraints on power distribution even at the SA level. We denote the maximum power accessible through the kth SA as P_k. Therefore, the total load at the kth SA should not exceed P_k.

The generation capability or the maximum power available from the grid forms another constraint on the power available for charging PEVs. We denote the total power available for charging (after removing the base load requirements) as P. The summation of the load due to all the vehicles that are charging should never exceed P.

2.2 Problem Formulation

We consider discrete charging intervals of 15 mins each, thus a full day has time slots between 0 and 96. The charging strategy, or scheduling, is done just before the beginning of the time interval and we assume that the total available power, P and the power accessible through the kth SA, P_k, are known a priori to the start of the scheduling process for the upcoming charging interval.

For a given time interval, the number of plugged in vehicles under the kth sub-aggregator and the total number of plugged in vehicles are given by N_k and N, respectively. $\mathcal{S}_k$ is the set of vehicles connected to kth SA and hence, $N_k = |\mathcal{S}_k|$

The objective of this study is to charge the vehicles which have the highest user-convenience. The user-convenience function here, as given by (2.1), represents the user's need for charging. Thus, by selecting the vehicles with the highest user-convenience for charging we are selecting the vehicles that require the charging interval the most. The function of (2.1) is a function of the state of charge (SOC) and the plug-off time.

$$J_{i,k} = \frac{SOC_{i,k}^{desired} - SOC_{i,k}^{current}}{L_{i,k} \cdot \max(1, t_{i,k}^{plug-off} - t_{curr})} \tag{2.1}$$

where $SOC_{i,k}^{desired}$ and $SOC_{i,k}^{current}$ represent the expected SOC at the plug-off time, $t_{i,k}^{plug-off}$, and the SOC at the current time, t_{curr}, respectively, for i-th PEV in k-th SA.

The numerator represents the difference between the desired and the current SOC at the given time slot. Its range is between 0 and 100. As the battery is charged, $SOC_{i,k}^{current}$ approaches $SOC_{i,k}^{desired}$ and the numerator approaches 0. The denominator represents the time remaining until plug-off time. The plug-off time is specified by the user. The denominator also includes $L_{i,k}$, the charging rate of the PEV. This has been included in the denominator to ensure that the value $J_{i,k}$ is the user convenience per unit power. The max operator is used to ensure that the denominator doesn't become negative in-case the user

leaves the PEV connected even after the plug-ff time.This user convenience function is thus bounded between a min and max value of 0 and 100, respectively.

During the course of this thesis different variants of the user convenience function were tried out but the one in (2.1) yielded the best results and thus all the case studies consider the user-convenience function given by (2.1).

The objective of charging the vehicles with the highest priorities is equivalent to maximizing the value of the cumulative priority function. This needs to be achieved while not exceeding the local and total power bounds. The cumulative priority function is given as:

$$\text{maximize:} \quad J = \sum_{k=1}^{K} \sum_{i=1}^{N_k} J_{i,k} L_{i,k} s_{i,k} \tag{2.2}$$

subject to

$$\sum_{i=1}^{N_k} s_{i,k} L_{i,k} \leq P_k \tag{2.3}$$

$$\sum_{k=1}^{K} \sum_{i=1}^{N_k} s_{i,k} L_{i,k} \leq P \tag{2.4}$$

For i-th PEV in k-th SA, $s_{i,k} \in \{0, 1\}$ denotes the charging variable. It can take only 2 values 0 or 1 representing either no charging or charging at the rated power $L_{i,k}$. $J_{i,k}$ is the user convenience function per unit power for the i-th PEV in the k-th SA. The constraints (2.4) and (2.3) formalize the restrictions on the total availability of power and the restrictions due to distribution. In detail, constraint (2.4) states that the total power to charge the PEVs cannot exceed the maximum power available from the feeder, while constraint (2.3) relates to the maximum power accessible to the k-th SA which takes into account the physical limitations. The constraint in (2.4) can be relaxed when $\sum_{k=1}^{K} P_k \leq P$. It is included to derive a complete solution when $\sum_{k=1}^{K} P_k \geq P$.

To solve this optimization in a centralized infrastructure, all the PEVs can report their values to the central aggregator and, then, the central aggregator can select the set of PEVs with the ψ highest priority values. Where, ψ is the maximum number of vehicles that can be charged while conforming to the power constraints.

In the proposed scheme this objective is achieved in a decentralized fashion. The kth SA has only $J_{i,k}$ values for $i \in \mathcal{S}_k$. Hence, a consensus based approach to exchange, $J_{i,k}$ values between SAs is put forth whose goal is to select vehicles from across the network such that (2.2) is asymptotically maximized. We will further elaborate about this in the following section.

2.3 Algorithm Description

To decentralize the process of maximizing the cumulative priority function of (2.2), each SA, needs the information about the $J_{i,k}$ values of all the connected PEVs. But as seen from Fig. 2.1 each SA is connected only to a subset of all the PEVs. Therefore to maximize (2.2), the kth SA should transmit $J_{i,k}$ for all $i \in \mathcal{S}_k$ to all the other SAs. Since each SA has N_k connected cars and hence N_k priority values (N_k can be of the order of few thousands to a few hundred thousands), transmitting and receiving such large quantities of data between SAs will be an intensive operation from the communication perspective and will not be practically feasible, especially when the SAs are not fully connected (see topology in Fig 2.1).

Hence, we discretize the possible values of $J_{i,k}$ and into M distinct levels and use the cardinality of these levels, instead of the individual values of $J_{i,k}$, for communication. The idea here is that now the kth SA can just share the cardinality of each level with the other SAs and hence all the SAs will be aware of the global cardinality of each level. This is achieved by an iterative consensus based approach. The global cardinality of a

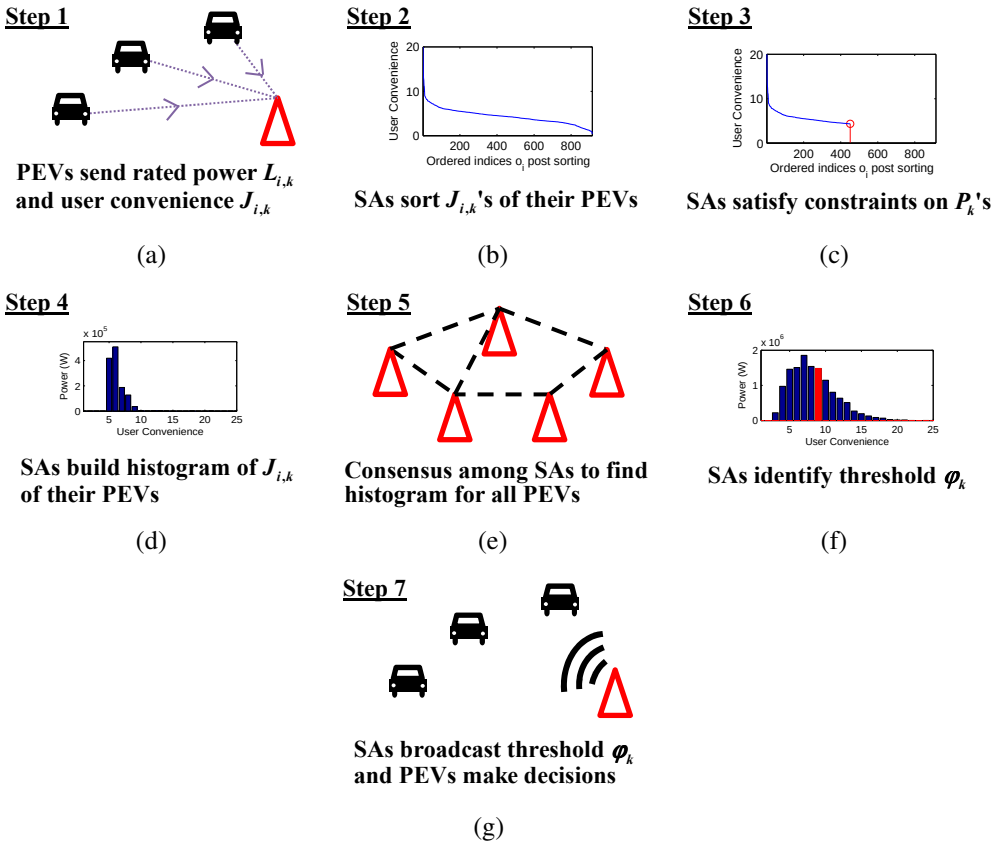

Figure 2.2. Summary of the proposed algorithm.

level is a measure of the number of vehicles whose priority values are represented by that level. After finding the global cardinality for each level, using consensus averaging [26], the task of maximizing (2.2) will boil down to selecting the vehicles whose priority value exceeds an appropriately selected threshold. To distribute the processing and to reduce communication, the SAs just broadcast the threshold to all the PEVs connected to them. The PEV then compares their $J_{i,k}$ value with the threshold and decide whether they can charge or not.

In detail the proposed algorithm involves the following steps:

1) Computation of user convenience value at each PEV: Each PEV $i \in \mathcal{S}_k$, connected to kth SA calculates the priority function $J_{i,k}$ (as given by (2.1) and transmits this value and the rated power $L_{i,k}$, to the kth SA, for all $k \in [1, K]$.

2) Sorting of Priority values at each SA: The SA $k \; \forall \; k \; \in \; [1, K]$ sorts the user-convenience values in a descending order. The ordered set of user-convenience values at the kth SA is denoted as.

$$\mathcal{P}_k = \left\{ J_{o_1,k}, J_{o_2,k}, \ldots, J_{o_i,k}, \ldots, J_{o_{N_k},k} \right\} \tag{2.5}$$

For which it holds that,

$$J_{o_i,k} \geq J_{o_{i+1},k}, \quad \forall i \in [1, N_k - 1] \tag{2.6}$$

While, o_1, o_2, o_{N_k} is the related ordering of the indexes representing the PEVs in $\mathcal{S}_k$.

3) Applying the Local Power Constraints: At the k-th SA, we use only the number of vehicles whose cumulative power requirements will not violate the local power limitations and thus truncate the ordered set $\mathcal{P}_k$ appropriately. Formally, if $\sum_{i=o_1}^{o_{N_k}} L_{i,k} > P_k$, the SA updates the set $\mathcal{P}_k$ as

$$\mathcal{P}_k = \left\{ J_{o_1,k}, J_{o_2,k}, \ldots, J_{o_{\tilde{N}_k},k} \right\}, \tag{2.7}$$

where $\tilde{N}_k$ fulfills the local power limitations, i.e.,

$$\sum_{i=o_1}^{o_{\tilde{N}_k}} L_{i,k} \leq P_k < \sum_{i=o_1}^{o_{\tilde{N}_k+1}} L_{i,k}. \tag{2.8}$$

This avoids exceeding the local power limitations without having any effect on the optimality of the solution as $\tilde{N}_k$ PEVs with the highest priority values are used by the SA for further computation.

4) Calculation of Bin and Histogram for User Convenience: The range of values of $J_{i,k}$, namely the interval $[J_{MAX}, J_{MIN}]$ is discretized into M bins to reduce the infinite possible values of user convenience into a finite set. The mth bin corresponds to:

$$b_m = [\underline{J} + (m-1)\Delta, \underline{J} + m\Delta] \tag{2.9}$$

where $\Delta = (\overline{J} - \underline{J})/M$ denotes the bin width. Then, the power requirement of the PEVs in each bin, b_m, is calculated at each SA first. Let $\mathcal{P}_{k,m}$ denote the user convenience values in the set $\mathcal{P}_k$ of the k-th SA which fall within the m-th bin, i.e.,

$$\mathcal{P}_{k,m} = \{J_{o_i,k} \in \mathcal{P}_k \text{ and } J_{o_i,k} \in b_m\} \tag{2.10}$$

with power requirement $\rho_{k,m} = \sum_{J_{i,k} \in \mathcal{P}_{k,m}} L_{i,k}$. Thus, it can easily be deduced that

$$\mathcal{P}_k = \bigcup_{m=1}^{M} \mathcal{P}_{k,m}. \tag{2.11}$$

5) Number of vehicles in b_m across SAs: This step entails determining the number of vehicles connected with their user-convenience value in the interval b_m. Since vehicles with $J_{i,k} \in b_m$ may be connected to different SAs, the SAs need to collaborate to determine the total population of vehicles in b_m, denoted as Γ_m.

This can be expressed by

$$\Gamma_m = \sum_{k=1}^{K} \rho_{k,m} = K\frac{1}{K}\sum_{k=1}^{K} \rho_{k,m} = K\bar{\Gamma}_m, \;\; m \in [1, M]. \tag{2.12}$$

At the kth SA, the $\Gamma_m \forall m \in [1, M]$ is estimated via the consensus iterates $\Gamma^{\tau}_{k,m}$ where τ denotes the consensus iteration index. Specifically, the iterates from [26] and the Metropolis-Hasting weights can be expressed as:

At the kth SA, for every element of $\rho_{k,m}$ we calculate weighted average given by

$$\hat{\Gamma}^{\tau+1}_{k,m} = (1-\delta)\hat{\Gamma}^{\tau}_{k,m} + \sum_{j \in \mathcal{N}_k} \hat{\Gamma}^{\tau}_{j,m} w_{k,j} \tag{2.13}$$

Where, $w_{k,j}$ corresponds to weights used at SA to linearly combine the local estimates $\hat{\Gamma}^{\tau}_{k,m}$ and is selected as.

$$w_{k,j} = \frac{1}{max(|\mathcal{N}_k|, |\mathcal{N}_j|)} \tag{2.14}$$

$$\delta = \sum_{j \in \mathcal{N}_k} w_{k,j} \tag{2.15}$$

While the estimates in are initialized as

$$\hat{\Gamma}^0_{k,m} = {}_{k,m} \tag{2.16}$$

$\mathcal{N}_k$ represents the set of connected, single hop neighbors, for the kth SA.

In practice, a certain number of iterations is required to reach consensus, i.e., the consensus procedure stops when each SA knows the total required power at bin m, Γ_m. Thus, the following stopping criterion is considered

$$\lfloor \hat{\Gamma}^\tau_{k,m} K \rceil = \lfloor \hat{\Gamma}^\tau_{k',m} K \rceil, \ \ \forall k, k' \in \{1, 2, ...K\}, \tag{2.17}$$

where $\lfloor \cdot \rceil$ denotes the rounding operation. It takes a finite number of iterations to satisfy the stopping criterion in (2.17) as will be shown later in the case studies.

6) Find Charging cut-off or threshold on the user-convenience value at k-th SA:

Each SA identifies a threshold φ_k on the user convenience value. The PEVs with the user convenience value greater than φ_k are permitted to charge.

First, each SA computes the cumulative required power,

$$C_m = \sum_{k=m}^{M} \Gamma_k, \tag{2.18}$$

to charge all PEVs whose user convenience values lie on the $M - m + 1$ rightmost bins. Then, assuming the available power P is known, each SA calculates the bin μ where the threshold φ_k lies as follows:

φ_k lies as follows:

$$\mu = \begin{cases} M, & C_M \geq P \\ m, & C_m \geq P \geq C_{m+1} \\ 1, & P \geq C_1 \end{cases}. \tag{2.19}$$

Thus all PEVs in bins with index greater than μ are allowed to charge, while only some PEVs in bin μ can charge. Since at any SA the exact user convenience values and charging rates of the PEVs from other SAs is not available, each SA can evaluate the power made available to bin μ as

$$\Psi_{k,\mu} = \frac{P - C_{\mu+1}}{\Gamma_\mu} \left(\sum_{J_{i,k} \in \mathcal{P}_{k,\mu}} L_{i,k} \right), \tag{2.20}$$

i.e., in proportion to the cumulative charging load of the PEVs in the μ-th bin of the SA. Then, the number $i^\star$ of PEVs that can charge from the μ-th bin of the k-th SA is evaluated as

$$\sum_{i=1}^{i^\star} L_{o_i,k} \leq \Psi_{k,\mu} < \sum_{i=1}^{i^\star+1} L_{o_i,k}. \tag{2.21}$$

Finally, the threshold φ_k, i.e., the control signal for PEVs in its area, is computed as

$$\varphi_k = L_{o_{i^\star},k}. \tag{2.22}$$

7) Charging Decision:

Each SA broadcasts the threshold φ_k to PEVs in its group. Then, each PEV makes a binary charging decision

$$s_{i,k} = \begin{cases} 1, & if \;\; J_{i,k} \geq \varphi_k \\ 0, & \text{otherwise} \end{cases}, \quad \forall k \in \{1, \ldots, K\}, i \in \mathcal{S}_k \tag{2.23}$$

to decide if the i-th PEV connected to the k-th SA is allowed to charge (when the user convenience $J_{i,k}$ is greater than the threshold φ_k) or not.

2.3.1 Optimality Analysis

The cumulative user convenience function J can be rewritten, by exploiting the information about the bin μ where the threshold φ_k lies, as

$$\begin{aligned} J = \sum_{k=1}^{K}\sum_{i=1}^{N_k} J_{i,k}L_{i,k}s_{i,k} \quad &= \sum_{k=1}^{K}\sum_{m=1}^{\mu-1}\sum_{J_{i,k}\in\mathcal{P}_{k,m}} J_{i,k}L_{i,k}s_{i,k} \\ &+ \sum_{k=1}^{K}\sum_{J_{i,k}\in\mathcal{P}_{k,\mu}} J_{i,k}L_{i,k}s_{i,k} \\ &+ \sum_{k=1}^{K}\sum_{m=\mu+1}^{M}\sum_{J_{i,k}\in\mathcal{P}_{k,m}} J_{i,k}L_{i,k}s_{i,k} \end{aligned} \tag{2.24}$$

Since bins $\{\mu+1, \mu+2, \ldots, M\}$ represent PEVs with higher $J_{i,k}$ that will be charged, and that the PEVs belonging to $\{1, 2, \ldots, \mu-1\}$ cannot be charged, the maximum J in (2.2) will be

$$\begin{aligned} \max(J) \quad &= \sum_{k=1}^{K}\sum_{m=\mu+1}^{M}\sum_{J_{i,k}\in\mathcal{P}_{k,m}} J_{i,k}L_{i,k} \\ &+ \max\left(\sum_{k=1}^{K}\sum_{J_{i,k}\in\mathcal{P}_{k,\mu}} J_{i,k}L_{i,k}s_{i,k}\right), \end{aligned} \tag{2.25}$$

where the max in (2.25) is found such that

$$\textstyle\sum_{k=1}^{K}\sum_{J_{i,k}\in\mathcal{P}_{k,\mu}} L_{i,k}s_{i,k} \leq P - C_{\mu+1}. \tag{2.26}$$

Instead, the proposed algorithm due to step (6) can achieve a maximum user convenience, $\max(J^{alg})$, given by

$$\begin{aligned} \max(J^{alg}) \quad &= \sum_{k=1}^{K}\sum_{m=\mu+1}^{M}\sum_{J_{i,k}\in\mathcal{P}_{k,m}} J_{i,k}L_{i,k} \\ &+ \sum_{k=1}^{K}\max\left(\sum_{J_{i,k}\in\mathcal{P}_{k,\mu}} J_{i,k}L_{i,k}s_{i,k}\right) \end{aligned} \tag{2.27}$$

which is different from (2.25) as each SA individually tries to maximize J for its local PEVs connected to it. Each maximization inside the sum in (2.27) is performed such that

$$\textstyle\sum_{J_{i,k}\in\mathcal{P}_{k,\mu}} L_{i,k}s_{i,k} \leq \Psi_{k,\mu}. \tag{2.28}$$

Considering (2.25) and (2.27), the following propositions can be derived.

Proposition 1. In a homogeneous scenario (where all PEVs have the same charging rate, i.e., $L_{i,k} = L, \forall i, k$), the proposed algorithm maximizes the user convenience in (2.2) asymptotically as the number of bins increases.

Proof: See Appendix A.

Proposition 2. In the general case of a heterogeneous scenario, as the number of bins increases, the proposed algorithm maximizes the user convenience in (2.2) asymptotically if the μ-th bin has only one PEV. Otherwise, a percentage optimality gap $\epsilon^{\%}$ is defined as

$$\epsilon^{\%} = \left\{ \max \left(\sum_{k=1}^{K} \sum_{J_{i,k} \in \mathcal{P}_{k,\mu}} J_{i,k} L_{i,k} s_{i,k} \right) - \sum_{k=1}^{K} \max \left(\sum_{J_{i,k} \in \mathcal{P}_{k,\mu}} J_{i,k} L_{i,k} s_{i,k} \right) \right\} \Big/ \max(J), \tag{2.29}$$

where the max operators are subject to (2.26) and (2.28), respectively.

Proof: See Appendix A.

It is worthy to note that the numerator of (2.29) depends only on the PEV selection from the μ-th bin and, hence, majority of PEVs have no impact on $\epsilon^{\%}$, while the denominator represents all the charging PEVs from a SA. Moreover, the sub-optimality related to the numerator corresponds to just one PEV per SA, i.e., a total of K PEVs in the whole power system. Therefore, as the number of PEVs being charged per SA increases, the optimality gap $\epsilon^{\%}$ goes to zero.

2.3.2 Recursive Bin Splitting

The proposed algorithm maximizes the objective function in (2.2) accurately as the number of bins, M, tends to infinity. However, this increases the complexity of the consensus procedure in step (5) of the algorithm. Moreover, such an increment of bins across the entire range $[\underline{J}, \overline{J}]$ is not necessary, since only a small interval of values around the un-

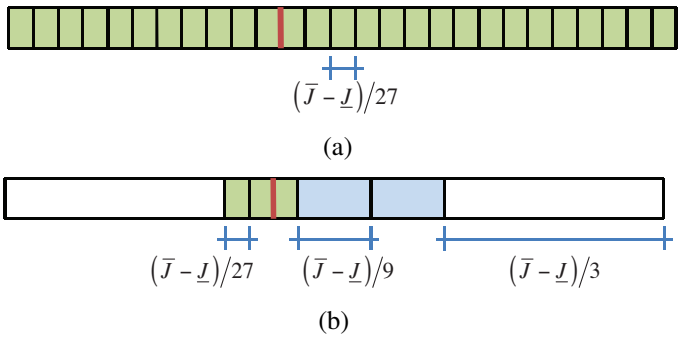

Figure 2.3. Example of division of the range between the maximum and minimum value of J with (a) normal procedure and (b) recursive approach. The red line represents the threshold.

known threshold φ_k is beneficial for the proposed algorithm's near optimality (or asymptotically exact in the homogeneous case).

A recursive approach is proposed to trade-off between the algorithm optimality and complexity. The idea is to recursively divide the range of user convenience values into a small number of bins, $\breve{M}$, moving towards the threshold φ_k at each recursion. Therefore, the number of bins around the threshold increases, decreasing the optimality gap, and ensuring asymptotic optimality in the homogeneous case. The sequential processing introduced by the recursive bin splitting may increase the execution time, but the number of computations and communicated data remains the same. However, one can note that this time increment is extremely small (order of seconds) compared to the time slot duration (order of minutes). It will be shown in Appendix B, that the optimal value of $\breve{M}$ for the recursive bin splitting is 3.

Fig. 3.2 illustrates the idea and the computational advantages of the recursive process. The basic procedure shown in Fig. 3.4 requires the simultaneous consensus on 27 bins. The recursive approach shown in Fig. 2.3(b) requires the consensus on only 9 bins and a triple execution time. Note that, in both scenarios, the final bin width is the same, i.e., $(\overline{J} - \underline{J})/27$.

2.4 Case Studies

2.4.1 Tracking an Arbitrary Charging Profile

The aim of this section is to show the ability of the proposed algorithm to track any given power profile specified by the grid operator. The algorithm treats the target profile as the total power available for charging, P. Each PEV is assumed to have a 12.5kWh battery with 0% initial SOC. The target SOC is 80% (i.e., a required charge of 10kWh for each PEV). Three possible charging rates are considered: (a) Level 1 charger with 1.4kW, (b) single-phase Level 2 chargers with 3.3kW, and (c) three-phase Level 2 chargers with 6.6kW [27]. Such charger types are considered for 40%, 40% and 20% of the PEVs, respectively. Finally, the value of $\overline{J} = 30/\underline{L}$ is considered, with $\underline{L}$ =1.4kW. A value of $30/\underline{L}$ is used instead of the earlier suggested $100/\underline{L}$ since it has been observed in the simulation that the user convenience never exceeds $30/\underline{L}$.

In Fig. 2.4(a), up-scaling the simulation setup in [14], 4000 PEVs are assumed to track a target profile with a certain regular shape. A total of 10 sub-aggregators are considered, each with 400 PEVs whose plug-in and plug-off times are uniformly distributed between 9:00-11:00 and 15:00-17:00, respectively. As can be seen from Fig. 2.4(a), the target profile is closely tracked and the power requirement never exceeds the available power. In the figure, a limited amount of power is not allocated and as a result the power profile with the proposed algorithm dips below the target profile between 16:00 hours and 17:00 hours, this is due to the absence of connected PEVs to charge. Another example with an arbitrary profile to track is illustrated in Fig. 2.4(b). Here, the profile shape is more variable than in the previous case. A population of 20000 PEVs connected from the first to the last time slot is considered. The profile obtained with the proposed distributed algorithm is the same as the target profile, demonstrating again the effectiveness of the proposed approach.

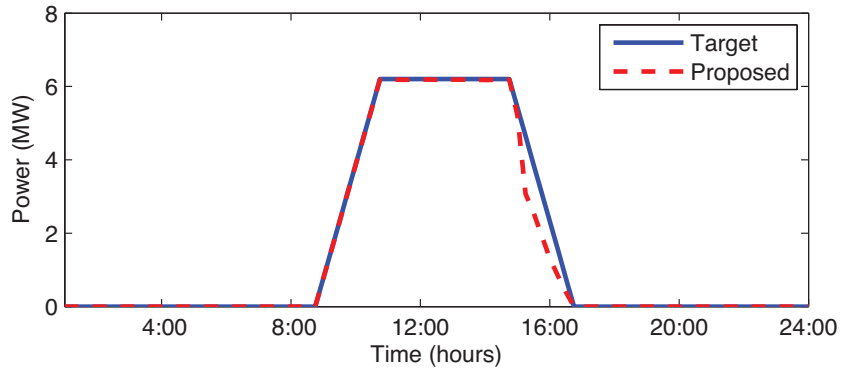

(a)

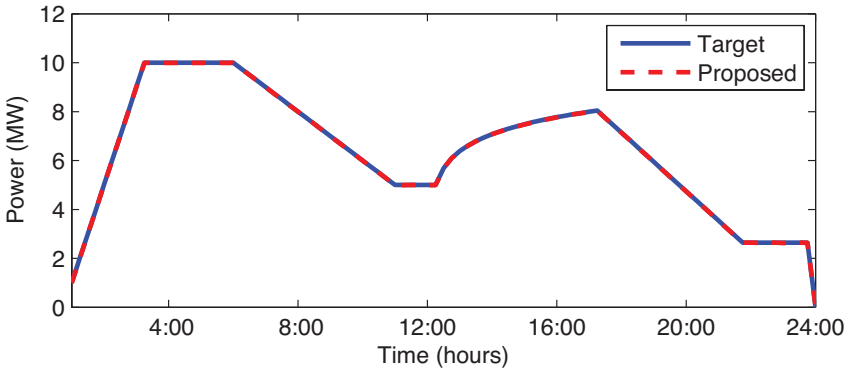

(b)

Figure 2.4. Tracking examples with two different profiles in (a) and (b).

To compare the solution obtained by the proposed algorithm with the optimal one, the *total optimality gap* (ϵ^{tot}) over a time horizon $[t_0, t_{fin}]$ is defined as a function of the optimality gap $\epsilon^{\%}(t)$ at time slot t in (2.29)

$$\epsilon^{tot} = \sum_{t=t_0}^{t_{fin}} w(t)\epsilon^{\%}(t), \tag{2.30}$$

with

$$w(t) = \frac{\min(P(t), L^{tot}(t))}{\sum_{t=t_0}^{t_{fin}} \min(P(t), L^{tot}(t))} \tag{2.31}$$

and

$$L^{tot}(t) = \sum_{k=1}^{K} \sum_{i=1}^{N_k} L_{i,k}. \tag{2.32}$$

Thus, the total optimality gap is the weighted average of the optimality gap at each time slot of the time horizon, where the weights are proportional to the power required to charge PEVs during the time slot.

For the considered case studies, the total optimality gap is a very small number. In detail, for the target profile in Fig. 2.4(a), mean and max total optimality gaps are a mere 0.04% and 0.09%, respectively, while for the case given in Fig. 2.4(b) they are 0.10% and 0.86%, respectively. Thus, the proposed distributed algorithm can effectively track any given profile. Moreover, compared to the existing approaches in [1] and [14] where the power profile of the coordinated charging can potentially go above the target profile to be tracked, the proposed solution guarantees that the coordinated charging profile with our algorithm never goes above the target profile. Such guarantees are necessary since in their absence the algorithms may potentially overload the system resulting into catastrophic outcomes.

2.4.2 Obtaining a Valley-filling Profile

The tracking capabilities of the proposed algorithm can be exploited to achieve a valley filling behavior, i.e., to schedule the PEVs during the night hours when the power cost is lower. This case study considers a residential setting with 10000 houses. The daily average load for the houses in the Southern California Edison area [28] is used to generate the base load profile. The set of PEVs includes sedans, compacts, and roadsters with a share of 40%, 40% and 20%, respectively. The batteries of sedans, compacts, and roadsters require 3, 8, and 12 hours of charging with a 3.3kW charger, respectively [27]. Charger types and distribution is the same as considered in the previous case study. Initial SOC is considered to be a Gaussian distributed random variable with mean at 0.5 and variance of 0.1 [15]. Plug-in and plug-off times are Gaussian distributed random variables with means at 5 PM and 7 AM (the next day), respectively, while their variances are considered to be 2

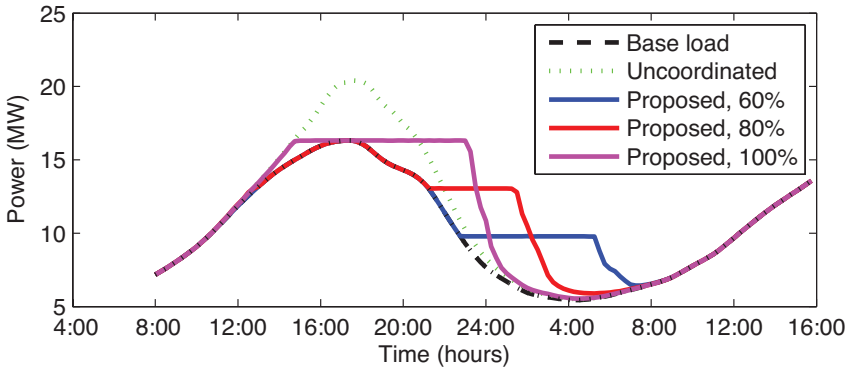

(a)

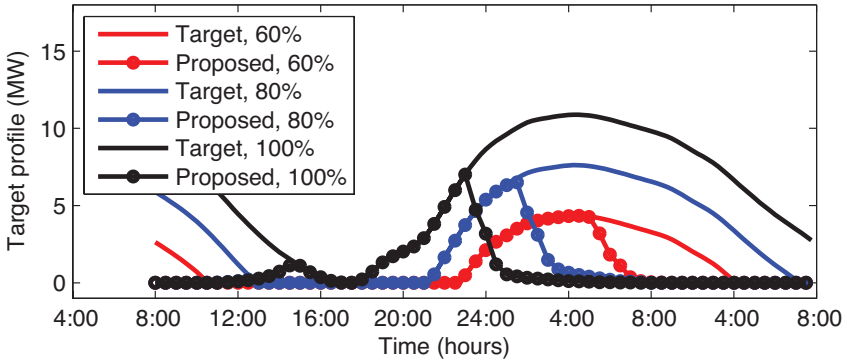

(b)

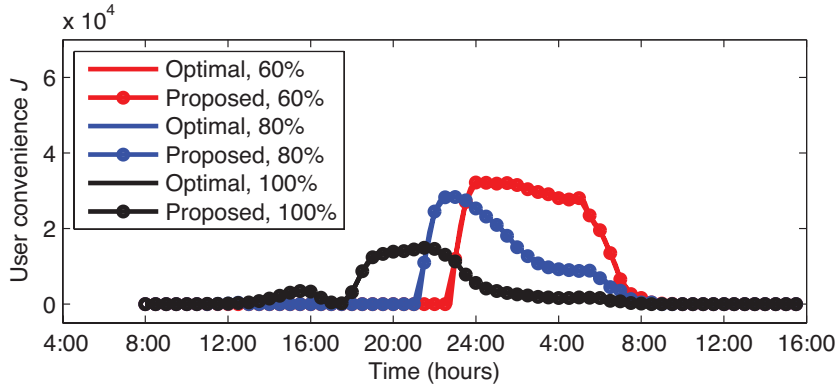

(c)

Figure 2.5. Example of obtaining a valley-filling behavior: (a) aggregated load profile including PEVs, (b) profile to track for PEV charging only, and (c) cumulative user convenience values.

hours and 1 hour, respectively [15]. The target SOC is 80%. The average number of PEVs per household is 1.86 based on the National Household Travel Survey [29].

A total of 10 sub-aggregators with 15%, 14%, 13%, 12%, 10%, 10%, 8%, 7%, 6%, 5% of the PEVs, respectively, are considered in this case study. The power constraints are in line with [1]. The constraints on total available power, P, is set as the maximum value of the base load curve. In detail, the local power constraints at each sub-aggregator, P_k, are set to be 25% larger than the mean power requirement across all sub-aggregators. On average, 10% of PEVs are connected to a sub-aggregator and, hence, P_k is the power required to charge 12.5% of PEVs.

In Fig. 2.5(a), the proposed algorithm is shown to allocate the PEVs load to non-peak periods, unlike the uncoordinated PEV charging that increases the peak load. This case study considers the scenario with 20% PEV penetration level and three different target profiles for the proposed algorithm. The three target profiles are considered to be 60%, 80%, and 100% of the peak base-load profile, respectively. As can be inferred from Fig. 2.5(a), the proposed algorithm closely follows the target profiles in all three cases. Indeed, in a practical scenario, the available power for PEV charging can be defined considering the generation capacity of the utility in conjunction with forecasts of base and PEV loads. Fig. 2.5(b) shows the three different target profiles to track for the proposed algorithm. The charging profile never exceeds the available power and closely follows the target profile. Thus, the proposed algorithm can be effectively exploited to obtain a valley filling profile. Finally, the cumulative user convenience value is illustrated in Fig. 2.5(c) for both the optimal case and the proposed algorithm, under different target profiles. These curves nearly overlap at all time instants. Thus, the proposed algorithm can achieve near-optimality in a heterogeneous setup, as also reported in Proposition 2.

Table 2.1. Comparison of SOC at different penetration levels with target SOC as 80%.

Penetration level	$Pr70$	$Pr75$	$Pr80$	$\overline{SOC}$	ϵ^{tot}
20%	99.92	99.75	99.44	79.98	0.22
50%	99.91	99.74	98.40	79.97	0.14
100%	93.68	81.91	52.45	77.44	0.10

Table 2.2. Comparison of SOC at different penetration levels with target SOC as 100%.

Penetration level	$Pr70$	$Pr80$	$Pr90$	$Pr100$	$\overline{SOC}$	ϵ^{tot}
20%	99.90	99.42	97.50	93.86	99.39	0.14
50%	99.87	99.01	94.06	74.99	98.20	0.08
100%	74.98	58.74	26.05	4.44	79.28	0.07

2.4.3 Numerical Performance

Table 2.1 and 2.2 present statistical information about the algorithm performance at 20%, 50%, and 100% PEV penetration levels with the target SOC of 80% and 100%, respectively. A target profile such that the aggregated profile does not exceed 100% of the peak of the base load profile has been considered. PrX represents percentage of PEVs with SOC greater than $X\%$ at the plug-off time, while $\overline{SOC}$ is the mean of the final SOC. The values obtained have been found over 100 runs of the algorithm. It is possible to note that the total optimality gap is about 0.1-0.2%, irrespective of the number of PEVs to charge. In the 20% penetration case, there are 3720 PEVs to be charged and almost all of them reach the target SOC of 80%. Similar results are reported for the 50% penetration case with 9300 PEVs. Even for the extreme case of 100% penetration, more than 90% of the PEVs achieve 70% SOC, with an average SOC of 77%, and with a negligible optimality gap of 0.10%. Naturally, not all PEVs achieve the target SOC due to the limited available power. For the 100% target SOC case with 20% and 50% PEV penetration levels, almost all PEVs reach the target SOC. Finally, it is worthy to note that the total optimality gap is even smaller for 100% target SOC compared to the previous case with 80% target SOC.

Table 2.3. Comparison of approximation error with different number of recursive bin splitting iterations.

Bin splitting iterations	**Actual bin number**	**Effective bin number**	**Mean** ϵ^{tot} (%)	**Max** ϵ^{tot} (%)
1	3	3	8.37	24.67
2	6	9	8.37	24.67
3	9	27	8.28	24.58
4	12	81	3.02	12.38
5	15	243	0.32	2.26
6	18	729	0.10	0.59

Table 2.3 shows that the recursive bin splitting reduces the difference between the optimal solution and the one achieved by the proposed algorithm, while linearly increasing the number of actual bins. Indeed, for a single splitting operation, the mean and maximum total optimality gaps are 8.37% and 24.67%, respectively. Instead, with 6 splitting operations, the number of actual bins is increased only to 18, while the mean and maximum total optimality gaps are reduced to the very small values of 0.10% and 0.59%, respectively.

2.4.4 Algorithm Complexity and Scalability

This section investigates the algorithm complexity by comparison with a distributed algorithm based on the well-known ADMM method [1]. Considering the distributed nature of the algorithms, it is worthy to note that the method in [1] requires a central aggregator in addition to the SAs, and it cannot guarantee the fulfillment of the power constraints (which are reported to be violated in 5% cases even after 60 iterations [1]). A summary of the required communications for both the proposed algorithm and [1] is summarized in Table 2.4, considering PEVs, SAs, and the central aggregator (AGG) for [1], where M is the number of bin splitting operations and I_1 is the number of iterations to reach consensus for the proposed algorithm, while I_2 is the number of ADMM iterations in [1].

Let us consider a case study with 20000 PEVs, equally distributed among 10 SAs, where each SA can communicate on average with a number of neighbor SAs, $\mathcal{N}$, equal to $|\mathcal{N}| = 4.8$. The proposed algorithm requires six bin splitting operations (i.e., $M = 18$) and 70 iterations ($I_1 = 70$) to reach a consensus on (2.12), while the work in [1] requires $I_2 = 60$ ADMM iterations. Note that the number of consensus iterations, I_1, for the proposed algorithm has been chosen equal to 70 since a campaign of experiments performed with random connections among the SAs has reported that 66 iterations are required on average. For every charging interval, at each SA, the proposed algorithm exchanges a total of 12×10^3 units of data with its neighbors, and receives 4×10^3 units of data from the PEVs, and broadcasts just one unit of data to the PEVs. The ADMM-based algorithm exchanges only 180 units of data with the central aggregator, but receives 1.2×10^5 units of data from the PEVs, and has to broadcast 120 units of data to the PEVs. Thus, one can note that the total amount of data required for both transmission and reception is about one order of magnitude less with the proposed algorithm compared to the ADMM-based algorithm in [1].

Finally, one can note that the communication overhead for the proposed approach is increased by only one transmission per PEV for every new PEV added. Indeed, the PEV parameters have to be sent to the SA only once during each time interval. On the other hand, the algorithm in [1] requires a communication overhead of the order of the number of ADMM iterations, I_2. Considering a typical value of $I_2 = 60$ [1], it is straightforward to note that the proposed approach exhibits a better scalability property compared to the literature. Thus, the order of the transmission data and the improved scalability shows the efficiency of the proposed distributed approach.

Table 2.4. Comparison of proposed algorithm and ADMM-based algorithm in [1].

Communications	**Proposed algorithm**	
	Transmission	**Reception**
At PEV	2 to SA	1 from SA
At SA	$M\|\mathcal{N}\|I_1$ to SAs 1 broadcast to PEVs	$M\|\mathcal{N}\|I_1$ from SAs $2N_k$ from PEVs
At AGG	none	none
Communications	**ADMM-based algorithm in [1]**	
	Transmission	**Reception**
At PEV	I_2 to SA	$2I_2$ from SA
At SA	I_2 to AGG $2I_2$ broadcast to PEVs	$2I_2$ from AGG N_kI_2 from PEVs
At AGG	$2KI_2$ to SAs	KI_2 from SAs

CHAPTER 3

CENTRALIZED AND DECENTRALIZED MINIMIZATION OF THE LOAD PEAK AND VARIANCE

In the previous chapter an algorithm that can efficiently track a utility specified load profile was introduced, but what are the possible and potentially ideal target load profiles and how can they be generated was not specifically discussed. Analyzing the PEV charge scheduling problem from the utility's perspective, the objective for the PEV charge scheduling process will be to minimize the variations in the load so that the power can be generated at a constant rate, thus maintaining a perfect balance between the demand and supply and in-turn reducing the production cost and ensuring minimal wastage. Schemes for achieving such minimum variance profiles have been explored in this chapter.

3.1 Problem Formulation

Two approaches to obtain a valley filling profile have been discussed here. In the former approach a centralized communication and distribution setup is used. The latter approach utilizes the scheme in Chapter 2 to achieve the valley filling objective in a decentralized setup.

For the centralized scheme a setup similar to the one in [15] is considered. It is assumed that all the PEVs are directly in contact with the central aggregator and request and receive permission to charge from it.

The objective here is to minimize the peak and variance of the aggregate load profile (aggregate load refers to the base load, $L_{base} = \{L_{base_{t_0}}, L_{base_{t_1}}, , L_{base_{t_{fin}}}\}$, and the PEV load). This is formulated as:

$$J = \underset{s_i(t)}{\operatorname{argmin}} \left(L_{var} + L_{peak}\right) \tag{3.1}$$

Where,

$$L_{var} = \frac{1}{t_{fin} - t_0} \sum_{t=t_0}^{t_{fin}} \left(L_{base}(t) + \sum_{i=1}^{N} L_i s_i(t) - \bar{L}\right)^2 \tag{3.2}$$

$$\bar{L} = \frac{1}{t_{fin} - t_0} \sum_{t=t_0}^{t_{fin}} \left(L_{base}(t) + \sum_{i=1}^{N} L_i s_i(t)\right)^2 \tag{3.3}$$

$$L_{peak} = \underset{t}{\operatorname{argmax}} \left(L_{base}(t) + \sum_{i=1}^{N} L_i s_i(t)\right) \tag{3.4}$$

t_0 and t_{fin} are the Time at which 1st PEV plugs-in and the last PEV plugs-off, respectively. $s_i(t)$ Charging variable for the i-th PEV at the time interval t and L_i is the charging load of the ith PEV. The charging process guarantees that all the PEVs will attain the target SoC (State of Charge).

From the discussion in Appendix C it can be seen that filling the valley from the lowest point is equivalent to variance minimization. Also, this means that variance minimization approach and valley filling approach inherently reduce the peak. Hence the simplified objective equation is expressed as:

$$J = \underset{s_i(t)}{\operatorname{argmin}} \left(L_{var}\right) \tag{3.5}$$

An intuitive scheduling algorithm would hence be to avoid any high points in the present load profile and schedule the charging during the lowest points of this profile. That is, if we need N time slots for charging the vehicle. We should choose the N lowest points on the present load curve. For this, the charging intervals for each PEV need to be explicitly identified. This scheduling can be done only for one PEV at a time. Hence, a priority or an order has to be set for each PEV to schedule. There are multiple ordering approaches

listed in [15]. But considering the target of valley filling, it is eminent that the scheduling is done such that the maximum number of time intervals with a high power requirement on the base load curve can be avoided. Therefore, some flexibility to move around the load curve to identify the lowest points and to schedule the charging during those intervals is required. This scheduling flexibility can be quantified as the number of extra slots each PEV has. i.e.

$$S_i^{ava} = \left\lfloor \frac{T_i^{plug-off} - T_i^{plug-in}}{T^{slot}} \right\rfloor \tag{3.6}$$

$$S_i^{req} = \left\lceil \frac{SOC_i^{desired} - SOC_i^{curr}}{T^{slot}} \right\rceil \tag{3.7}$$

$$S_i^{extra} = S_i^{ava} - S_i^{req} \tag{3.8}$$

Where $SOC_i^{desired}$ and SOC_i^{curr} represent the expected SOC at the plug-off time, $T_i^{plug-off}$, and the SOC at the current time, T^{curr}, respectively, for i-th PEV. T^{slot} refers to the time slot length. A time slot of 15 minutes has been considered in the current formulation. Since S_i^{extra} is bounded by the time a PEV is plugged in, it can be assumed to be in the range $\{1, 2, .., 96\}$, where 1 represents a connection time of 15 minutes and 96 represents the upper limit of 24 hours.

The higher the value of S_i^{extra}, the more is the scheduling flexibility. Vehicles with high flexibility can help achieve the valley filling behavior because they can schedule their charging during intervals with the lowest load. Therefore we choose the vehicles with low flexibility to schedule there charging periods first and later the higher flexibility vehicles are allowed to schedule. This scheduling is repeated, every time frame, until all of the vehicles are connected. And post that, the decided schedule is followed.

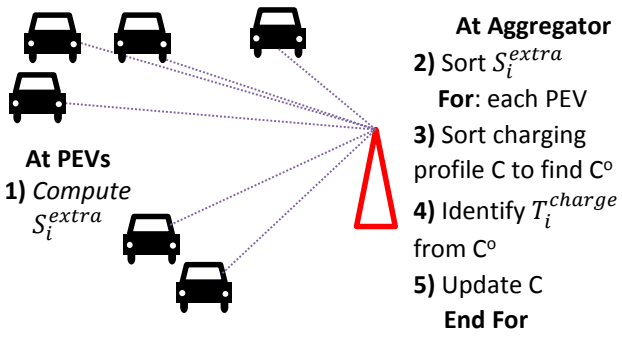

Figure 3.1. Summary of the proposed centralized valley-filling algorithm.

3.2 Algorithm 1: centralized

1. Each PEV calculates S_i^{extra} and transmits S_i^{req} and S_i^{extra} to the central aggregator.
2. The central aggregator sorts the PEVs into bins, b_m, based on their S_i^{extra} value.

$$b_m = \{\bigcup_i S_i^{extra} | S_i^{extra} = m\} \tag{3.9}$$

PEVs belonging to the bin with the lowest index m are allowed to schedule their charging first.

3. At the first time-slot, the aggregator initializes the present load profile, C, to the base load profile and, sequentially, identifies the scheduling slots for each PEV belonging to B_m, starting from $m = 1$. The present load refers to the sum of the base load and the anticipated charging load of the PEVs scheduled up to now, $C = \{C_{t_0}, C_{t_1}, ..., C_{t_{fin}}\}$. The present load at p^{th} time-slot is C_{t_p}.

The aggregator forms the sub-set $\mathcal{C}$ from the set C, and sorts it in an ascending order to form the set $\mathcal{C}^o$:

$$\mathcal{C} = \{C_{t_{curr}}, C_{t_{curr+1}}, ..., C_{t_{fin}}\}, \tag{3.10}$$

$$\mathcal{C}^o = \{C_{t_{o_{curr}}}, C_{t_{o_{curr+1}}}, ..., C_{t_{o_{fin}}}\}. \tag{3.11}$$

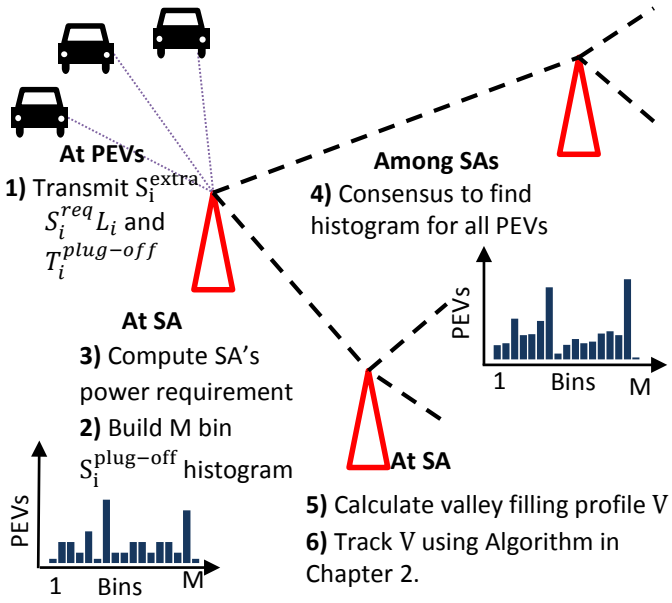

Figure 3.2. Summary of the proposed decentralized valley filling algorithm.

t_{curr} is the current time-slot, and $C_{t_{o_p}} \leq C_{t_{o_{p+1}}}$. Then, the set of time-slots during which the i^{th} PEV, with $S_i^{extra} \in \mathcal{B}_m$, is allowed to charge is defined as

$$T_i^{charge} = \{t_{o_{curr}}, t_{o_{curr+1}}, ..., t_{o_{S_i^{req}}}\}. \tag{3.12}$$

The charging schedule, T_i^{charge}, is sent to the respective PEV and the present load profile is finally updated to reflect the PEVs schedule and charging requirements.

$$C_{t_{o_p}} = C_{t_{o_p}} + L_i, \forall t_{o_p} \in T_i^{charge}. \tag{3.13}$$

4. The aggregator iterates step 3 for all sets of $\mathcal{B}_m$'s by increasing m until all PEVs are scheduled.

3.3 Algorithm 2: Decentralized

In the decentralized approach, a setup similar to the one in Chapter 2 is discussed. PEVs are divided amongst disjoint groups, each represented by a SA. The SA is considered

to be the local communication and power hub. It communicates only with the PEVs in its respective group and with some of the neighboring SAs in the power distribution network.

The sub-aggregators first reach a consensus on the total power demand and then identify a valley filling profile to track. Then, the algorithm discussed in Chapter 2 is used to charge the PEVs while tracking the generated valley filling profile.

1. Each PEV calculates S_i^{extra} and $S_i^{req}L_i$. It then transmits these values and $T_i^{plug-off}$ to their respective sub-aggregator (SA).
2. Each SA builds a M bin histogram of $S_i^{plug-off}$. Since the PEVs mainly plug-off during the morning hours, the M can be made a small number. The height of the histogram represents the number of PEVs with the particular plug-off slot and is given by $h_{m,k}$. The plug off slot is expressed as:

$$S_i^{plug-off} = \lfloor \frac{T_i^{plug-off}}{T^{slot}} \rfloor \tag{3.14}$$

3. Each SA then identifies the local energy requirement or energy demand as:

$$P_k^{total} = \sum_{i \in N_k} S_i^{req} L_i \tag{3.15}$$

Where N_k represents the set of PEVs connected to the kth SA. For simplicity, we assume that all the PEVs have the same charger type $L_i = L$ and hence P_k^{total} is considered as:

$$P_k^{total} = \sum_{i \in N_k} S_i^{req} L \tag{3.16}$$

4. The SAs then exchange $M + 2$ scalar with the neighboring SAs to reach a consensus on the magnitudes of the $M + 2$ elements across the entire network. The first M scalars represent the number of PEVs in each bin of the histogram, the $M + 1$th

element, $h_{m+1,k} = P_k^{total}$ and the $M+2$th element is the number of plugged-in PEVs N_k.

Let H_m represent the global value of the mth scalar across the network and can be expressed as:

$$H_m = \sum_{k=1}^{K} h_{m,k} = K\frac{1}{K}\sum_{k=1}^{K} h_{m,k} = K\bar{H}_m \tag{3.17}$$

for $m \in [1, M+2]$. Thus, each SA can evaluate H_m by computing H_m in a distributed fashion by using the consensus averaging algorithm in [26].

5. All the SAs know the total energy requirement from H_{M+1} and thus, the total number of slots required for charging all the PEVs is $\frac{H_{M+1}}{L}$. Using this, a valley filling profile, $V = \{V_{t_{curr}}, V_{t_{curr+1}}, , V_{t_{t_{fin}}}\}$ is found, where t_{curr} is the current time slot. V is initialized as the base load, L_{base}, and updated for each of the $\frac{H_{M+1}}{L}$ required charging slots based on the following rule:

$$V_i = \underset{i}{\operatorname{argmin}}\, V_i + L \tag{3.18}$$

s.to

$$V_i \leq (H_{M+2} - \sum_{c=t_{curr}}^{i} H_c)L + L_{base_i} \tag{3.19}$$

6. The updated profile $V = \{V_{t_{curr}}, V_{t_{curr+1}}, , V_{t_{t_{fin}}}\}$ is used for tracking by the decentralized tracking algorithm presented in Chapter 2. For the current tracking scenario the plug-off time slot, $S_i^{plug-off}$, is used as the user convenience function.

Both the above mentioned algorithms achieve aggregate load profile that display valley filling behavior. The aggregate load profile for some cases is discussed in the next section.

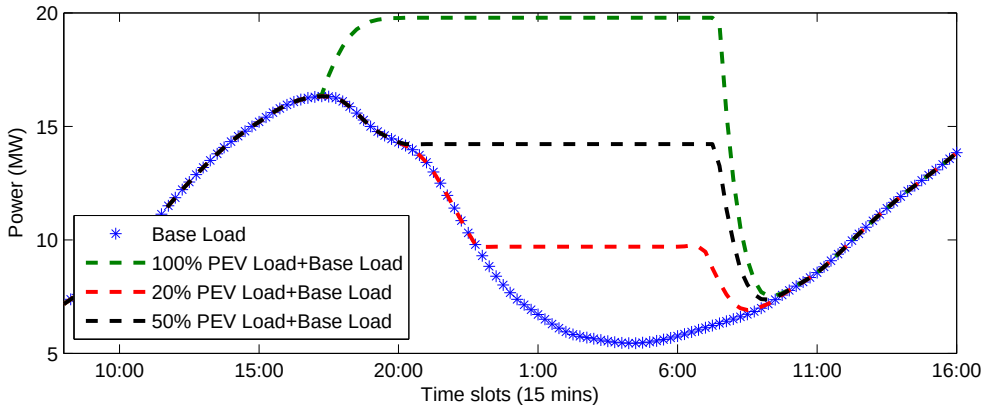

Figure 3.3. Aggregate load profiles for the centralized valley filling algorithm at 20%, 50%, 100% PEV penetration levels..

3.4 Case Study

The resedential setting discussed in Section 2.4 is used here. The aggregate load profiles, obtained by the centralized valley filling algorithm for 20%, 50%, 100% PEV penetration levels, are shown in Fig. 3.3.

CHAPTER 4

IMPACT OF CHARGING INTERRUPTION ON VALLEY FILLING BEHAVIOR AND VARIANCE MINIMIZATION

The objective of a coordinated charging process is to fill the valley of the load profile seen by the grid [30], i.e., minimize the variance of the aggregated load profile given by PEV and non-PEV loads. The charging process can be formulated, temporally, as an interrupted or uninterrupted charging process with PEVs being charged at the maximum rated power. In the interrupted charging scenario (also referred to as on-off charging [13]), a PEV is charged at discrete time-slots that may be separated by idle slots. In the uninterrupted charging scenario, the PEVs are charged continuously until they obtain their desired state of charge (SOC) [15]. Both scheduled charging scenarios are presented in Fig. 4.1. For the interrupted charging process, the PEV scheduling has the flexibility to charge during the time-slots with the lowest base load, while the uninterrupted charging does not have such flexibility. In this chapter, we study both scenarios from the perspective of their impact on the aggregated load profile and the aim of the coordinated charging strategies (i.e., variance minimization).

4.1 Charging Strategies

As described in the previous Chapter, the primary objective of the PEV charging strategy is to minimize the variance of the aggregated load profile:

$$min : \mathcal{J} = \frac{1}{(t_{fin} - t_0)} \sum_{t=t_0}^{t_{fin}} (L^{base}(t) + \sum_{i=1}^{N} L_i s_i(t) - \bar{L})^2 \tag{4.1}$$

where

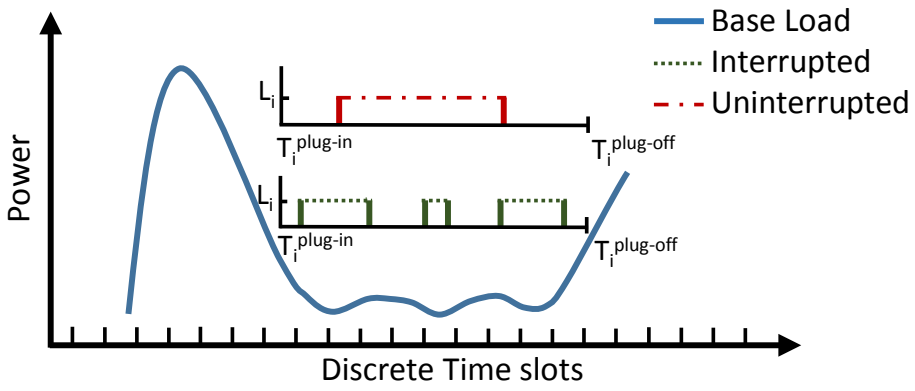

Figure 4.1. Scheduling in interrupted and uninterrupted charging scenarios for a sample base load profile. $T_i^{plug-in}$ and $T_i^{plug-off}$ are the plug-in and plug-off times of the i-th PEV and L_i is its charging rate.

$$\bar{L} = \frac{1}{(t_{fin} - t_0)} \sum_{t=t_0}^{t_{fin}} (L^{base}(t) + \sum_{i=1}^{N} L_i s_i(t)). \tag{4.2}$$

t_0 and t_{fin} are the first and the last time-slots, respectively. The minimization in (4.1) is with respect to $s_i(t)$ which denotes the binary charging decision for the i^{th} PEV during time-slot t. L_i is the charging power for the i^{th} PEV.

Scheduling the charging process during the time-slots where the present load is at its lowest value would decrease the variance of the load profile the most. Thus, the scheduling process may be seen as a sequential task in which a priority value, S_i, shall be assigned to each PEV to order the scheduling process. There are various approaches to prioritize the PEVs (e.g. [15]). The earliest deadline first (EDF) policy gives priority to schedule PEVs with the earliest plug-off time $T_i^{plug-off}$. The shortest job first (SJF) policy prioritizes the PEVs with the shortest charging time $S_i^{SJF} = \frac{SOC_i^{desired} - SOC_i^{curr}}{L_i T^{slot}}$, where $SOC_i^{desired}$ and SOC_i^{curr} represent the expected SOC at $T_i^{plug-off}$ and the SOC at the current time T_{curr} for the i^{th} PEV, respectively. T_{slot} refers to the duration of each time-slot. The least slack time (LST) policy gives priority to the PEVs with the smallest slack time $S_i^{slack} = S_i^{ava} - S_i^{req}$, as discussed in Section 3.1.

In this Chapter, the uninterrupted charging process has been implemented in line with the process suggested by the authors in [15] and the interrupted charging process discussed in Section 3.2 has been considered.

4.2 Case Study

The residential setting in Section 2.4 is used here. A time-slot of 15 minutes has been considered; The time horizon of 24 hours is discretized to $\{1, 2, ..., 96\}$. The aggregate load profiles, obtained by the interrupted and uninterrupted charging processes for 30% PEV penetration level, are shown in Fig. 4.2. The change in the variance of the aggregated load profile for the two charging processes is illustrated in Fig. 4.3. The difference in the variance decreases with the increase in PEV penetration levels for all the considered scheduling policies. At lower penetration levels, the difference in the variances of the aggregated load profiles obtained by the interrupted and uninterrupted charging processes is relevant. Even at the 30% penetration level, a 15% difference between the interrupted and uninterrupted scenarios can be observed. One can then conclude that for lower penetration levels it is better to adopt a charging scheduling based on interrupted profiles, while for greater penetration levels, an uninterrupted strategy may provide similar performances compared to the interrupted strategies. It can be inferred from Fig. 4.2 that the performance of the three scheduling schemes (i.e. SJF, EDF and LST) are similar as the three curves overlap with each other.

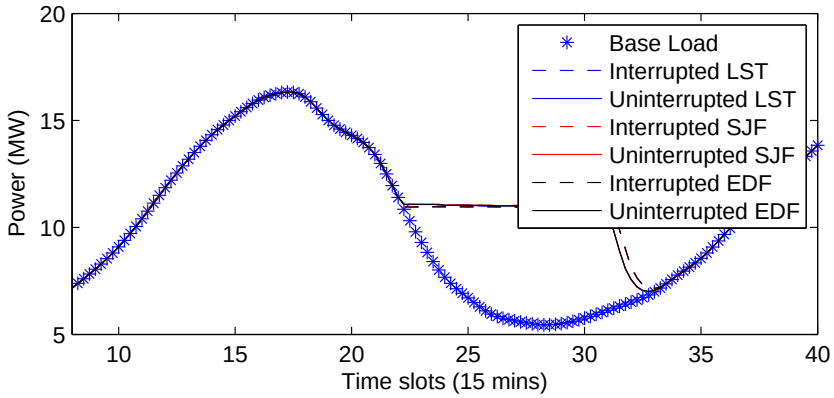

Figure 4.2. The load curves obtained at 30% PEV penetration.

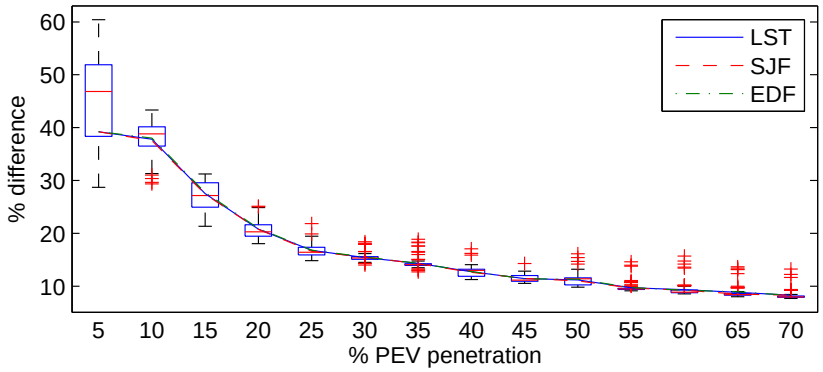

Figure 4.3. Percentage difference in variance values between uninterrupted and interrupted charging scenarios. The figure is a box plot with the central red mark as the median and the edges of the blue box marking the 25th and 75th percentiles of the percentage difference. The whiskers extending beyond the box mark the most extreme data points which are not considered as outliers.

CHAPTER 5

CONCLUSION

The thesis analyzes different aspects of the coordinated PEV charging problem. First, a distributed algorithm for PEV coordinated charging is proposed to maximize the user convenience under the power constraints imposed by the power utility. It is shown that the algorithm can track any given power profile provided by the power utility, while maximizing the user satisfaction in terms of state of charge and charging time. The work discusses and tackles many practical limitations like the heterogeneity in the charging rates. This has been included to incorporate PEVs charging process at residence, parking lots, or charging stations, into a unified coordination framework. Moreover, discrete charging rates have been considered to accommodate for the limitation imposed by the charger technologies. Most importantly, the algorithm is implemented in a distributed fashion by exploiting consensus algorithms for inter-sub-aggregator communications, thus making it is easily scalable and tolerant to network faults.

The objective of minimizing the load variance and peak has been discussed next. Theoretical proof has been provided to prove that the variance minimization incorporates peak minimization and thus the objective function can be simplified. A very intuitive centralized scheduling algorithm has been proposed and a decentralized algorithm (that builds on the previously developed algorithms) to achieve similar results was discussed next.

Lastly, the impact of interrupted and uninterrupted charging strategies on the aggregate load profile has been discussed. It is shown that at low penetration level (up to 30%), the variance of the aggregated load profile is further reduced using the interrupted charging

process. It is also shown that the priority assignment schemes have no impact on the the load variance.

The effectiveness of the algorithms proposed here has been demonstrated in realistic scenarios, with a heterogeneous PEV population, under different penetration levels.

APPENDIX A

OPTIMALITY ANALYSIS

A.1 Proof of Proposition 1

Let us consider the asymptotic behavior, i.e., $M \to \infty$, in the simplified case of a homogeneous scenario. Each bin b_m has bin-width $\Delta \to 0$, and every user convenience value in $[\underline{J}, \overline{J}]$ is represented by a distinct bin. Considering (2.25) and (2.27), one can note that the optimality depends only on the sub-selection in μ-th bin. Let η_μ be the PEV number in μ-th bin, then the following two cases may be verified.

A.1.1 $\eta_\mu = 1$

The only PEV in bin μ, say $\tilde{i}$, is assumed to be connected to SA $\tilde{k}$. Then, from (2.25), it follows

$$\max \left(\sum_{k=1}^{K} \sum_{J_{i,k} \in \mathcal{P}_{k,\mu}} J_{i,k} L_{i,k} s_{i,k} \right) = J_{\tilde{i},\tilde{k}} L_{\tilde{i},\tilde{k}} \tag{A.1}$$

and, from (2.27), it follows

$$\sum_{k=1}^{K} \max \left(\sum_{J_{i,k} \in \mathcal{P}_{k,\mu}} J_{i,k} L_{i,k} s_{i,k} \right) = J_{\tilde{i},\tilde{k}} L_{\tilde{i},\tilde{k}}, \tag{A.2}$$

under the constraints in (2.26) and (2.28), respectively. Thus, the proposed algorithm achieves the result in (A.2) which is equal to the optimal one in (A.1).

A.1.2 $\eta_\mu > 1$

The μ-th bin has more than one PEV, thus sub-selection is required. However, since all PEVs in μ-th bin have the same user convenience values, any of them can be selected without affecting the result. Thus, the proposed algorithm is also optimal in this case.

A.2 Proof of Proposition 2

Let us consider the asymptotic behavior in the general case of heterogeneous scenario. Similar to the previous proof, two cases are considered.

A.2.1 $\eta_\mu = 1$

The argument presented in Appendix A.1.1 is repeated, and the optimal solution is achieved by the proposed algorithm.

A.2.2 $\eta_\mu > 1$

Optimality gap ϵ in (2.29) directly follows from (2.25) and (2.27).

APPENDIX B

OPTIMAL NUMBER OF BINS

We demonstrate that the optimal number of bins $\breve{M}$ for the recursive bin splitting operation is 3. Let x and y denote the number of recursions and bins, respectively. If the consensus averaging is done for a maximum of M bins, it is required to maximize $y = (\breve{M})^x$ under the constraint that $x \cdot \breve{M} = M$. Then,

$$ln(y) = \frac{M}{\breve{M}} ln(\breve{M}) \tag{B.1}$$

Differentiating both sides yields

$$\frac{1}{y}\frac{dy}{d\breve{M}} = -\frac{M}{\breve{M}^2} ln(\breve{M}) + \frac{M}{\breve{M}^2} \tag{B.2}$$

$$\frac{dy}{d\breve{M}} = \frac{M}{\breve{M}^2}[1 - ln(\breve{M})]\breve{M}^{M/\breve{M}} \tag{B.3}$$

Setting $dy/d\breve{M} = 0$ and finding the maximum of the cost function leads to

$$\frac{M}{\breve{M}^2}[1 - ln(x)]\breve{M}^{M/\breve{M}} = 0. \tag{B.4}$$

Considering finite values of $\breve{M}$ yields

$$1 - ln(\breve{M}) = 0, \text{and } \breve{M} = e. \tag{B.5}$$

Since $\breve{M}$ should be an integer we set the number of bins for the recursive bin splitting operation is 3, i.e., the closest integer to e.

APPENDIX C

VARIANCE MINIMIZATION ENSURES PEAK MINIMIZATION

To Prove:

Variance minimization is equivalent to filling the valley from the lowest point.

OR

In the context of PEV Charging, variance minimization is equivalent to scheduling the PEV charging during the time slots where the present-load is the least.

Let x(t) represent the present load at time slot t.

For simplicity we consider that only one PEV is connected for charging and it needs only one time slot to charge. This assumption can be made without any loss of generalization as the process can be repeated for other PEVs after updating the present load.

Variance of present load:

$$v = \frac{1}{N} \sum_{t=t_{curr}}^{t_{fin}} (x(t) - \overline{x})^2 \tag{C.1}$$

Where,

$$\overline{x} = \frac{1}{N} \sum_{t=t_{curr}}^{t_{fin}} x(t) \tag{C.2}$$

Let the load profile post scheduling the PEV charging be $\widehat{x(t)}$

$$\overline{\widehat{x(t)}} = \frac{1}{N} \sum_{t=t_{curr}}^{t_{fin}} \widehat{x(t)} \tag{C.3}$$

$$\widehat{v} = \frac{1}{N} \sum_{t=t_{curr}}^{t_{fin}} (\widehat{x(t)} - \overline{\widehat{x}})^2 \tag{C.4}$$

Since the PEV charging requires only one time slot to charge,

$$\overline{\widehat{x(t)}} = \frac{1}{N} \sum_{t=t_{curr}}^{t_{fin}} \widehat{x(t)} = \frac{1}{N} \sum_{t=t_{curr}}^{t_{fin}} x(t) + \frac{L_i}{N} = \overline{x} + \frac{L_i}{N} \tag{C.5}$$

Where, L_i the charging rate of the PEV.

Now we have,

$$v = \widehat{v} + \beta \tag{C.6}$$

The new charging slot is selected such that the new variance v is minimized and therefore, should be maximized. We had,

$$\widehat{v} = \frac{1}{N} \sum_{t=t_{curr}}^{t_{fin}} (\widehat{x(t)} - \overline{\widehat{x}})^2 \tag{C.7}$$

$$\begin{aligned} \widehat{x} &= x(t) \forall t \in \{[t_{curr}, t_{fin}] - \{k\}\} \\ &= x(t) + L_i \ \ for \ \ t = k \end{aligned} \tag{C.8}$$

From (C.5) we have, $\overline{\widehat{x}} = \overline{x} + \frac{L_i}{N}$

$$\widehat{v} = \frac{1}{N} \Bigg(\Bigg(\sum_{t=t_{curr} t \neq k}^{t_f in} (x(t) - \overline{x} - \frac{L_i}{N})^2 \Bigg) + (x(k) + L_i - \overline{x} - \frac{L_i}{N})^2 \Bigg) \tag{C.9}$$

Substituting from (C.1) and (C.2) and solving we get

$$\widehat{v} = v + c_1 + 2(x(k) - \overline{x}) \tag{C.10}$$

Where,

$$c_1 = \frac{L_i^2}{N^2}(N-1) \text{ is a constant} \tag{C.11}$$

Comparing (10) and (6) we have

$$\beta = -(c_1 + 2\Delta(x(k) - \overline{x})) \tag{C.12}$$

As stated before, the objective is to maximize β. As can be seen β is a function of k. Therefore, we must choose k in order to maximize β.

$$\underset{k}{\operatorname{argmax}}\, \beta = \underset{k}{\operatorname{argmax}}\{-(c_1 + 2\Delta(x(k) - \overline{x}))\} \tag{C.13}$$

$$= \underset{k}{\operatorname{argmin}}\, c_1 + 2\Delta(x(k) - \overline{x}) \tag{C.14}$$

Since, c_1 and 2δ are constants they can be removed from the equation.

$$= \underset{k}{\operatorname{argmin}}\{x(k) - \overline{x}\} \tag{C.15}$$

Also, for a given present load profile, $x(t), \overline{x}$ is a constant.

Therefore,

$$= \underset{k}{\operatorname{argmin}}\{x(k)\} \tag{C.16}$$

Hence, we choose k that has the minimum value $x(k)$. That is, we choose the minima of the present load profile, $\operatorname{argmin}_k\{x(k)\}$, as the time slot for charging the PEV.

REFERENCES

[1] C.-K. Wen, J.-C. Chen, J.-H. Teng, and P. Ting, "Decentralized plug-in electric vehicle charging selection algorithm in power systems," *IEEE Transactions on Smart Grid*, vol. 3, no. 4, p. 17791789, Dec. 2012.

[2] T. R. Hawkins, B. Singh, G. Majeau-Bettez, and A. H. Strømman, "Comparative environmental life cycle assessment of conventional and electric vehicles," *Journal of Industrial Ecology*, vol. 17, no. 1, pp. 53–64, 2013.

[3] Benefits and considerations of electricity as a vehicle fuel. [Online]. Available: http://www.afdc.energy.gov/fuels/electricity_benefits.html

[4] P. Denholm and W. Short, "An evaluation of utility system impacts and benefits of optimally dispatched plug-in hybrid electric vehicles," *National Renewable Energy Laboratory, Tech. Rep. NREL/TP-620-40293*, 2006.

[5] K. Parks, P. Denholm, and A. J. Markel, *Costs and emissions associated with plug-in hybrid electric vehicle charging in the Xcel Energy Colorado service territory*, 2007.

[6] S. Shafiee, M. Fotuhi-Firuzabad, and M. Rastegar, "Investigating the impacts of plug-in hybrid electric vehicles on power distribution systems," *IEEE Transactions on Smart Grid*, vol. 4, no. 3, pp. 1351–1360, September 2013.

[7] L. Pieltain Fernandez, T. G. S. Roman, R. Cossent, C. M. Domingo, and P. Frias, "Assessment of the impact of plug-in electric vehicles on distribution networks," *IEEE Transactions on Power Systems*, vol. 26, no. 1, pp. 206–213, Feb. 2011.

[8] Q. Gong, S. Midlam-Mohler, V. Marano, and G. Rizzoni, "Study of PEV charging on residential distribution transformer life," *IEEE Transactions on Smart Grid*, vol. 3, no. 1, pp. 404–412, Mar. 2012.

[9] E. Veldman and A. Verzijlbergh, "Distribution grid impacts of smart electric vehicle charging from different perspectives," *IEEE Transactions on Power Systems*, vol. 6, no. 1, pp. 333–342, January 2015.

[10] Z. Ma, I. Hiskens, and D. Callaway, "A decentralized MPC strategy for charging large populations of plug-in electric vehicles," in *18th IFAC World Congress*, 2011, pp. 10 493–10 498.

[11] C. Ahn, C. T. Li, and H. Peng, "Optimal decentralized charging control algorithm for electrified vehicles connected to smart grid," *Journal of Power Sources*, vol. 196, no. 23, pp. 10 369–10 379, Dec. 2011.

[12] W. Su and M. Y. Chow, "Performance evaluation of an EDA-based large-scale plug-in hybrid electric vehicle charging algorithm," *IEEE Transactions on Smart Grid*, vol. 3, no. 1, pp. 308–315, Mar. 2011.

[13] Q. Li, T. Cui, R. Negi, F. Franchetti, and M. Ilic, "On-line decentralized charging of plug-in electric vehicles in power systems," *arXiv:1106.5063v2 [math.OC]*, 2011.

[14] L. Gan, U. Topcu, and S. Low, "Optimal decentralized protocol for electric vehicle charging," *IEEE Transactions on Power Systems*, vol. 28, no. 2, pp. 940–951, May 2013.

[15] G. Binetti, A. Davoudi, D. Naso, B. Turchiano, and F. L. Lewis, "Scalable real-time electric vehicles charging with discrete charging rates," *IEEE Transactions on Smart Grid*, vol. 6, no. 5, pp. 2211–2220, Sep. 2015.

[16] L. Zhang, F. Jabbari, T. Brown, and S. Samuelsen, "Coordinating plug-in electric vehicle charging with electric grid: Valley filling and target load following," *Journal of Power Sources*, vol. 267, pp. 584–597, 2014.

[17] N. Chen, C. W. Tan, and T. Q. S. Quek, "Electric vehicle charging in smart grid: optimality and valley-filling algorithms," *IEEE Journal of Selected Topics in Signal Processing*, vol. 8, no. 6, pp. 1073–1083, Dec. 2014.

[18] A. Di Giorgio, F. Liberati, and S. Canale, "Electric vehicles charging control in a smart grid: a model predictive control approach," *Control Engineering Practice*, vol. 22, pp. 147–162, Jan. 2014.

[19] T. M. Bandhauer, S. Garimella, and T. F. Fuller, "A critical review of thermal issues in lithium-ion batteries," *Journal of the Electrochemical Society*, vol. 158, no. 3, pp. R1–R25, 2011.

[20] L. Gan, U. Topcu, and S. H. Low, "Stochastic distributed protocol for electric vehicle charging with discrete charging rate," in *2012 IEEE Power and Energy Society General Meeting*, 2012, pp. 1–8.

[21] S. Han, S. Han, and K. Sezaki, "Development of an optimal vehicle-to-grid aggregator for frequency regulation," *IEEE Transactions on Smart Grid*, vol. 1, no. 1, pp. 65–72, Jun. 2010.

[22] Y. He, B. Venkatesh, and L. Guan, "Optimal scheduling for charging and discharging of electric vehicles," *IEEE Transactions on Smart Grid*, vol. 3, no. 3, pp. 1095–1105, Sept 2012.

[23] D. Wu, D. C. Aliprantis, and L. Ying, "Load scheduling and dispatch for aggregators of plug-in electric vehicles," *IEEE Transactions on Smart Grid*, vol. 3, no. 1, pp. 368–376, Mar. 2012.

[24] V. Robu, S. Stein, E. H. Gerding, D. C. Parkes, A. Rogers, and N. R. Jennings, "An online mechanism for multi-speed electric vehicle charging," in *Auctions, Market Mechanisms, and Their Applications*. Springer, 2012, pp. 100–112.

[25] O. Ardakanian, S. Keshav, and C. Rosenberg, "Real-time distributed control for smart electric vehicle chargers: From a static to a dynamic study," *IEEE Transactions on Smart Grid*, vol. 5, no. 5, pp. 2295–2305, Sep. 2014.

[26] L. Xiao and S. Boyd, "Fast linear iterations for distributed averaging," in *42nd IEEE Conference on Decision and Control*, 2003, pp. 4997–5002.

[27] A. Ipakchi and F. Albuyeh, "Grid of the future," *IEEE Power and Energy Magazine*, vol. 7, no. 2, pp. 52–62, Mar. 2009.

[28] South California Edison (SCE) website. [Online]. Available: www.sce.com

[29] US Department of Transportation. 2009 National Household Travel Survey. [Online]. Available: http://nhts.ornl.gov/2009/pub/stt.pdf

[30] Z. Ma, D. S. Callaway, and I. A. Hiskens, "Decentralized charging control of large populations of plug-in electric vehicles," *IEEE Transactions on Control Systems Technology*, vol. 21, no. 1, pp. 67–68, Jan. 2013.

BIOGRAPHICAL STATEMENT

Akshay Malhotra received his B.Eng from the P.E.S Institute of Technology, Bangalore, India in 2011. From July 2011 to Dec 2013 he worked at Ittiam Systems, Bangalore, India. Since January 2014, he has been working towards his Masters in Science in the Department of Electrical Engineering at the University of Texas at Arlington, TX, USA. His research focuses on distributed signal processing, wireless sensor networks and electric vehicle charging strategies.